PHYSICAL REVIEW B VOLUME 23, NUMBER 4 15 FEBRUARY 1981

Line shape of the low-energy tail of exciton absorption in molecular crystals

Jai Singh
Research School of Chemistry, Australian National University, Box 4, P.O. Canberra A.C.T. 2600, Australia
(Received 21 November 1979)

The influence of crystal defects and phonons on the line shape of the low-energy tail of exciton absorption is calculated for molecular crystals with the lower limit of their exciton band at $\vec{k} = 0$. The exciton Hamiltonian for a crystal with lattice defects is derived from that for a perfect crystal with lattice vibrations. Calculation of the line shape is done assuming that the individual lattice defects have independent effects on the unperturbed exciton band. Three examples of the molecular exciton energy bands are considered: (1) one-dimensional tight-binding exciton band, (2) the exciton bands with Hubbard's model of density of states, and (3) exciton bands with density of states independent of the exciton energies. At very low temperatures where the influence of the defects is dominant, we have found the asymmetric low-energy tail due to defects, acting as shallow traps, in all the three examples. The observed asymmetric line shape in 1,2-dibromonaphthalene single crystals is, therefore, attributed to such shallow traps and analogous to the Urbach-Martienssen tail observed in alkali halides. As the temperature increases and phonons become more active, the line shape becomes symmetric due to the dominant influence of thermal broadening.

I. INTRODUCTION

Exciton scattering by chemical impurities, lattice imperfections, and phonons is intimately concerned in energy transport processes in molecular crystals and can, in principle, be studied through spectroscopic properties. The observations of asymmetric line shapes at low temperatures in dibromonaphthalene (DBN) single crystals[1,2] in form similar to that of the Urbach-Martienssen (UM) rule[3,4] followed in alkali halide crystals suggests further investigation into the theory of exciton absorption line shape in molecular crystals, in order to extract information from band profiles bearing on the underlying scattering. It is rather common to find the minimum of the exciton band in organic cyrstals at $\vec{k} = 0$.[1] Here the usual theory of line shape of absorption[5-6] is not applicable. The vanishing density of states beyond the band edges of the unperturbed exciton band creates a difficulty in finding well-defined energy states at $\vec{k} = 0$.[5] Sumi and Toyozawa[7] suggest that the asymmetric line shapes are primarily due to the scattering of excitons by lattice vibrations at the band edge ($\vec{k} = 0$) in alkali halide crystals. In molecular crystals, however, the asymmetric line shapes are observed at very low temperatures (0–2 K) where the scattering of excitons by thermally excited phonons cannot play a large role. Where the crystal has more than one molecule per unit cell, so that each molecular transition gives more than one exciton branch, exciton-phonon scattering can occur via interbranch coupling, even at the lowest temperature, but the broadening away from the phononless transition is very slight.[8] Larger asymmetry is expected to be either intrinsic with the crystal, arising from impurities and defects, or characteristic of the excitation, as, for example, caused by local lattice deformation resulting from the excitation of a particular molecular site. It is important to distinguish between these sources of asymmetry.

Klafter and Jortner[9] proposed that the asymmetric line shape can arise from microscopic structural disorder in pure molecular crystals. In their model Hamiltonian, Klafter and Jortner introduce an additional term associated with a distribution of molecular excitation energies caused by variation of the dispersion interaction. In other words, although the crystal lacks gross dislocation and other forms of disorder, there is a sufficient fluctuation of structural parameters at lattice points to give a spread of energies. They assume that this variation follows a Gaussian distribution with an energy width less than that of the original exciton band.

Recently we calculated the effect of lattice defects (not impurities) on the low-energy tail of the line shape of exciton absorption for crystals with the minimum of the unperturbed exciton band at $\vec{k} = 0$.[10] The Hamiltonian for such a crystal is derived from the exciton Hamiltonian for a perfect crystal with lattice vibrations and is different from that considered by Klafter and Jortner. The modified Hamiltonian thus obtained contained an additional term for the energy changes caused by defects.

In this paper we use the same modified Hamiltonian[10] but apply a different method to calculate the low-energy tail of exciton absorption. We consider a class of organic crystals with the exciton state ($\vec{k} = 0$) at the lower extreme of the exciton band. Essentially the same results are obtained if this state lies at the top band edge. The asymmetric tail will then be on the high-energy side and for

that reason, hard to observe. We begin in Sec. II with the derivation of the Hamiltonian of an exciton interacting with phonons and lattice defects which destroy the translational symmetry of the crystal. The additional operator of the exciton-defect interaction thus obtained is then removed by diagonalizing the Hamiltonian in Sec. III. In Sec. IV we calculate the Green's function of the diagonalized part of the Hamiltonian (with no exciton-phonon interaction operator) and derive the line-shape function of the low-energy tail outside the unperturbed exciton band. Two specific examples of crystals are considered: (1) Crystals in which the molecular interactions are very much stronger in one crystal direction than in any other so that the band structure is nearly that of a one-dimensional lattice. An example is in the triplet state of DBN. (2) Three-dimensional crystals with unperturbed exciton bands having (a) the Hubbard[11] type of density of states, and (b) the density of states independent of exciton energy. In Sec. V we consider the complete Hamiltonian including exciton-phonon interaction as well, for calculating the exciton propagator and then the line shape of the low-energy tail.

For one-dimensional crystal with nearest-neighbor coupling we find that the low-energy tail exhibits an exponential rise with steepness parameter, $\sigma = B/D^2$, as independent of temperature, B being the half-width of the unperturbed exciton band and D that of the distribution of the defective-site energies. In crystals with other band structures the low-energy tail shows behavior between Gaussian and exponential.

In Sec. V it is shown how the presence of defects modifies the exciton-phonon interaction operator. The line shape due to thermal broadening is also modified; no asymmetry is, however, produced in the line shape. The theory is developed primarily to study the influence of lattice defects due to the displacements of equilibrium of lattice sites. This can, however, be used for studying the influence of impurities equally well. We expect the simple model system to help the understanding of the UM tail (asymmetric line shape) observed in molecular crystals.

II. HAMILTONIAN

The Hamiltonian $\hat{H}$ for a Frenkel exciton interacting with the lattice vibrations of a perfect molecular crystal is written in a single-phonon approximation as[12]

$$\hat{H} = \sum_n [\Delta\epsilon + D(0)] B_n^\dagger B_n + \sum_{n,m}{}' M_{nm}(0) B_n^\dagger B_m + \sum_{s,\vec{q}} \hbar\omega_s(\vec{q})(b_{\vec{q}s}^\dagger b_{\vec{q}s} + \tfrac{1}{2}) + \sum_{n,m}{}' B_n^\dagger B_m \Big[\sum_{j=1}^{6} \Big(R_n^j \frac{\partial}{\partial R_n^j} + R_m^j \frac{\partial}{\partial R_m^j}\Big) M_{nm}(R)\Big]_0 + \sum_{n,m}{}' B_n^\dagger B_n \Big[\sum_{j=1}^{6} \Big(R_n^j \frac{\partial}{\partial R_n^j} + R_m^j \frac{\partial}{\partial R_m^j}\Big) D_{nm}(R)\Big]_0 . \tag{2.1}$$

$\Delta\epsilon$ is the free-molecule exciton energy, $D(0)$ is the lattice dispersion energy change on molecular excitation at the undisplaced lattice site, M_{nm} is the resonance coupling energy between sites n and m, D_{nm} is the dispersion energy term, $\omega_s(\vec{q})$ is the frequency of the phonon mode $\vec{q}$ in the s branch, and R_n^j is the jth displacement of molecule n.

We model the defective crystal as follows. A number n_d out of the total N lattice sites are assumed to be displaced from their equilibrium positions. Such defects are intrinsic to the crystals, usually built in at the time of crystal growth. The energy required to produce and maintain the displaced equilibrium structure is, therefore, ignored in our discussion. We use only the fact that, in this structure, the exciton-lattice interactions are changed in the ground and excited states sothat the displaced molecules can act as exciton traps to the extent that their excitation energies have been changed. The displacement at the pth site will be taken to have six components, three in translation and three in rotation: the latter are about the principal axes of the molecule concerned. Replacing thus R_p^j by $R_p^j + \rho_p^j$ in (2.1), we find the Hamiltonian $\hat{H}_d$ for the defective crystal as (2.2):

$$\hat{H}_d = \hat{H} + \Delta\hat{H}, \tag{2.2}$$

where

$$\Delta\hat{H} = \sum_{p=1}^{n_d} \sum_{m\neq p} \sum_{j=1}^{6} \rho_p^j \Big(\frac{\partial D_{pm}(R+\rho)}{\partial R_p^j}\Big)_0 B_p^\dagger B_p + \tfrac{1}{2} \sum_{p=1}^{n_d} \sum_{m\neq p} \sum_{j=1} \rho_p^j \Big(\frac{\partial M_{pm}(R+\rho)}{\partial R_p^j}\Big)_0 B_p^\dagger B_m + \text{H.c.}, \tag{2.3}$$

p stands for a defective site. The resonance integrals M_{pm} will be assumed to change so little that their contribution to $\hat{H}_d$ can be neglected so that the Hamiltonian (2.3) remains as[13] (2.4):

$$\hat{H}_d = \hat{H} + \sum_p^{n_d} \Delta_p B_p^\dagger B_p, \tag{2.4}$$

where

$$\Delta_p = \sum_{m\neq p} \sum_{j=1}^{6} \rho_p^j \Big(\frac{\partial D_{pm}(R+\rho)}{\partial R}\Big)_0 . \tag{2.5}$$

In first-order perturbation theory we regard the wave functions as those for the unperturbed problem, i.e., those for the perfect lattice, and transform the operators according to[12]

$$B_n = N^{-1/2} \sum_{\vec{k}} B_{\vec{k}} e^{i\vec{k}\cdot\vec{n}}, \tag{2.6}$$

$$R_n^j = \left(\frac{\hbar}{2I_j N \Omega_s(\vec{q})}\right)^{1/2} \sum_{\vec{q}} e_s^j(\vec{q}) \phi_s(\vec{q}) e^{i\vec{q}\cdot\vec{n}}, \tag{2.7}$$

where

$$\phi_s(\vec{q}) = (b_{\vec{q}s} + b_{-\vec{q}s}^{\dagger}).$$

Using (2.6) and (2.7) in (2.4) we find

$$\begin{aligned}\hat{H}_d = &\sum_{\vec{k}} E(\vec{k}) B_{\vec{k}}^{\dagger} B_{\vec{k}} + N^{-1} \sum_{k,k'} \sum_{p}^{n_d} \Delta_p e^{i(\vec{k}'-\vec{k})\cdot\vec{p}} B_{\vec{k}}^{\dagger} B_{\vec{k}'} \\ &+ \sum_{\vec{q}} \hbar\omega(\vec{q}) (b_{\vec{q}}^{\dagger} b_{\vec{q}} + \tfrac{1}{2}) \\ &+ N^{-1/2} \sum_{\vec{k},\vec{q}} [F(\vec{k},\vec{q}) + \chi(\vec{q})] B_{\vec{k}+\vec{q}}^{\dagger} B_{\vec{k}} (b_{-\vec{q}}^{\dagger} + b_{\vec{q}}).\end{aligned} \tag{2.8}$$

The index s for the phonon branches is dropped in (2.8). Except for the second term which represents the exciton-defect interaction, expression (2.8) is the usual Hamiltonian in $\vec{k}$ space[14,15] of an exciton interacting with phonons.

For calculating the energy shift and line-shape function of exciton absorption due to the presence of lattice defects, it should be possible in principle to evaluate the Green's function of (2.8) by applying the method used by Iguchi[16] and Craig and Dissado.[14] The evaluation of Green's function in this way, however, is complicated by the cross products arising from the exciton-defect and exciton-phonon interaction operators. We will, therefore, first of all diagonalize the Hamiltonian part ($\hat{H}_d'$) consisting of only the first two terms of (2.8). In the previous paper[10] this diagonalization involved only a single impurity in the crystal. Here we will follow the procedure of Craig and Philpott.[17]

III. DIAGONALIZATION OF $\hat{H}_d'$

We start with

$$\hat{H}_d' = \sum_{\vec{k}} E(\mathrm{k}) B_{\vec{k}}^{\dagger} B_{\vec{k}} + N^{-1} \sum_{\vec{k},\vec{k}'} \sum_{p}^{n_d} \Delta_p e^{i(\vec{k}'-\vec{k})\cdot\vec{p}} B_{\vec{k}}^{\dagger} B_{\vec{k}'}, \tag{3.1}$$

and expand the crystal wave function of an exciton with energy E in terms of localized and delocalized basis sets as

$$|\Psi\rangle = \sum_n a_n(E) B_n^{\dagger} |0\rangle \tag{3.2}$$

and

$$|\Psi\rangle = \sum_{\vec{k}} A_{\vec{k}}(E) B_{\vec{k}}^{\dagger} |0\rangle, \tag{3.3}$$

where

$$a_n(E) = N^{-1/2} \sum_{\vec{k}} A_{\vec{k}}(E) e^{i\vec{k}\cdot\vec{n}}. \tag{3.4}$$

The ground state $|0\rangle$ of the crystal used in (3.2) and (3.3) is defined as that in which all the molecules in the crystal are in their ground states.

We solve the Schrödinger equation

$$\hat{H}_d' |\Psi\rangle = E |\Psi\rangle, \tag{3.5}$$

by making use of (3.2), and obtain the equation (3.6):

$$[E - E(\vec{k})] A_{\vec{k}}(E) - N^{-1} \sum_{\vec{k}'} \sum_{p} \Delta_p e^{i(\vec{k}'-\vec{k})\cdot\vec{p}} A_{\vec{k}}(E) = 0. \tag{3.6}$$

From (3.3), (3.4), and (3.6) we then find

$$\sum_{p} \left(a_n \delta_{n,p} - N^{-1} \sum_{\vec{k}} \frac{\Delta_p a_p}{E - E(\vec{k})} \right) e^{i\vec{k}\cdot(\vec{n}-\vec{p})} = 0. \tag{3.7}$$

If we assume that each defect affects the crystal levels independently of the effect of the others, which is an acceptable approximation, the secular equation (3.7) reduces, for $n = p$, to

$$1 - N^{-1} \sum_{\vec{k}} \frac{\Delta_p}{E - E(\vec{k})} = 0. \tag{3.8}$$

As a result of our approximation of noninteracting impurities, the secular equation (3.8) is the same as the well-known result for a single impurity.[10,17,18]

The energy eigenvalue spectrum of an exciton in a crystal with defective sites is obtained by solving the secular equation (3.8). The eigenvalue obtained from (3.8) is, however, a function of Δ_p of a single defective site, and in view of (3.7) similar eigenvalues will be obtained corresponding to every Δ_p. The eventual diagonal form of the Hamiltonian (3.1) will be written as

$$\hat{H}_d' = \sum_{p}^{n_d} \hat{H}_d'^{p}, \tag{3.9}$$

where

$$\hat{H}_d'^{p} = \sum_{\alpha(p)} E_\alpha B_\alpha^{\dagger} B_\alpha. \tag{3.10}$$

E_α denotes the αth eigenvalue obtained from the secular equation (3.8) for a single Δ_p, and $B_\alpha^{\dagger}$ is the corresponding transformed creation operator of an exciton with E_α given by

$$B_\alpha^{\dagger} = \sum_{\vec{k}} A_{\vec{k}}(\alpha) B_{\vec{k}}^{\dagger}, \tag{3.11}$$

where $A_k(\alpha)$ is derived within the single-site approximation as

$$\begin{aligned} A_{\vec{k}}(\alpha) &= N_\alpha^{-1} \exp(i\vec{k}\cdot\vec{p}) [E - E(\vec{k})]^{-1}, \\ N_\alpha &= \left(\sum_{\vec{k}} [E - E(\vec{k})]^{-2} \right)^{1/2}. \end{aligned} \tag{3.12}$$

IV. THE LOW-TEMPERATURE EXCITON LINE SHAPE DUE TO CRYSTAL DEFECTS

Equation (3.8) may be solved numerically in cases where the energies $E(\vec{k})$ are known as a function of $\vec{k}$ or as individual values. Here, however, we take three models of exciton bands where $E(\vec{k})$ is a known function of $\vec{k}$, and where analytical solutions of (3.8) are possible. The two cases are (1) crystals in which the band structure is essentially one-dimensional, as in the triplet state of DBN,[1] and (2) crystals where the energy density of states may be taken to be (a) of the Hubbard type[11] and (b) independent of energy.

A. Crystals with one-dimensional band structure

The unperturbed exciton band in one-dimensional crystals can be written as

$$E(k)=A+B\cos k, \tag{4.1}$$

with B taken to be negative; the minimum of $E(k)$ is at $k=0$ and the maximum at $k=\pm\pi$. The unperturbed bandwidth is $2B$. The value of A (4.1) simply determines the energy of the band center, and we may take it that $A=0$.

Our aim is to study the line shape of absorption at the band edges. It depends on levels displaced outside the exciton band, with energies E found by solving (3.8). For an infinite crystal the sum over k in (3.8) can be converted into an integral which gives, through (4.1), the unperturbed energy Green's function as

$$G_0(E)=N^{-1}\sum_{k}[E-E(\vec{k})]^{-1}=(1/2\pi)\int_{-\pi}^{\pi}\frac{dk}{E-B\cos k+i\epsilon}$$

$$=P_0(E)+i\pi N_0(E)=(E^2-B^2)^{-1/2}, \tag{4.2b}$$

where $P_0(E)$ is the principal value of $G_0(E)$ and $N_0(E)$ is the unperturbed density of states.

From (3.8) and (4.2b) we then find

$$(E^2-B^2)^{1/2}=\Delta_p \quad \text{or} \quad E=\pm(B^2+\Delta_p^2)^{1/2}. \tag{4.3}$$

For each Δ_p there are two possible energy eigenvalues, E, symmetrically below and above the unperturbed band. The structure of (3.8) shows that for $\Delta_p<0$ (i.e., defect sites for which the excitation energy is less than the normal) we find energy levels below the band ($E<B<0$) and for $\Delta_p>0$ they are above the band ($E>0$). We consider only levels below, contributing to the long-wave band edge, with energy $E=B(1+\Delta_p^2/B^2)^{1/2}$.

To get the line shape of the low-energy tail of absorption we need transition moment and the density of states as a function of E. If we denote by $T_d(E_\alpha)$ the transition moment to the state at E_α, then following Craig and Philpott[17] we will have for a single-defect site in the crystal

$$T_d(E_\alpha)=\frac{T}{E_\alpha-E(0)}\left(\sum_k[E_\alpha-E(\vec{k})]^{-2}\right)^{-1/2}, \quad E_\alpha<B, \tag{4.4}$$

T being the perfect-crystal transition moment and $E(0)$ the energy of the unperturbed exciton at $k=0$. In case of infinite one-dimensional crystals the summation inside the large parentheses of (4.4) can again be evaluated as an integral to give

$$T_d(E_\alpha)=\frac{T}{E_\alpha-B}\left(\frac{NE_\alpha}{(E_\alpha^2-B^2)^{3/2}}\right)^{-1/2}, \quad E_\alpha<B. \tag{4.5}$$

Inasmuch as there is one defect, and therefore only a single level displaced out of the band, the density of states is a delta function at E_α, following formally from the imaginary part of the energy Green's function $G(E,E_\alpha)$:

$$G(E,E_\alpha)=(E-E_\alpha+i\epsilon)^{-1}, \quad \epsilon\to 0. \tag{4.6a}$$

This gives for the density of states $N_\alpha(E_\alpha)$,

$$N_\alpha(E_\alpha)=\frac{1}{\pi}\,\mathrm{Im}G(E,E_\alpha)=\delta(E-E_\alpha). \tag{4.6b}$$

The intensity of absorption is proportional to the product of $T_d(E_\alpha)^2$ and $N_0(E_\alpha)$. The absorption line shape $[I_d(E)]$ due to a number n_d of isolated noninteracting defects is then written as

$$I_d(E)\propto-\sum_{p}^{n_d}T_d^2(E_{\alpha(p)})N_\alpha(E_{\alpha(p)})$$

$$=-\frac{T^2}{N}\left(\frac{(E+B)^3}{E^2(E-B)}\right)^{1/2}\sum_p\delta(E-E_{\alpha(p)}), \quad E<B. \tag{4.7}$$

The low-energy tail consists of delta-function absorption peaks equal to the number of defects.

We notice that the limiting value of $T_d(E_\alpha)$ in (4.4) as E_α approaches the band edge is equal to the perfect-crystal transition moment T. The same must of course be true of the integral form of intensity given in (4.7). However, (4.5) contains explicitly the number N of molecules in the crystal, whereas in (4.4) it is implicit only as the number of terms in the sum. The intensity in (4.7) is most conveniently expressed in terms of the intensity per molecule through the relation $T=N^{1/2}m$, m being the free-molecule moment.

To illustrate the intensity outside the band for defective crystals, we take two cases: (1) all defect sites have the same depth Δ and (2) the depths are distributed according to a Gaussian function.

1. Identical Δ for all defect sites

Here $I(E)$ (4.7) is independent of p:

$$I_d(E)=-n_d\vec{m}^2[(E+B)^3/E^2(E-B)]^{1/2}\delta(E-E_\alpha). \tag{4.8}$$

The low-energy "tail" has a single delta-function peak with the intensity of absorption proportional to the number of defects. For large Δ this peak will be well separated from the original exciton band.

For deep traps, which leave the band levels unperturbed, we see from (4.8) that each trap molecule contributes its own intensity. For shallower traps, each contributes a larger amount. Thus in a band for which $B=-200\ \mathrm{cm}^{-1}$, a trap of depth $\Delta=-100\ \mathrm{cm}^{-1}$ produces an out-of-band level $-23\ \mathrm{cm}^{-1}$ to the side of the band edge, with an absorption corresponding to 8.1 molecular absorptions and a consequent reduction in absorption to levels on the band. In a crystal with one such trap per thousand molecules and an optical density of 3 units in the pure-crystal absorption region, the trap optical density would be about 0.9, and readily observable.

2. *Gaussian distribution of depths*

The Gaussian distribution for Δ was first proposed by Sumi and Toyozawa[7] in connection with asymmetric line shapes arising from exciton-phonon interactions in alkali halide crystals. Following Sumi and Toyozawa, Klafter and Jortner[9] assumed that the change in the dispersive interaction due to the excitation of molecules also follows the Gaussian distribution, and they averaged the energy Green's function calculated from their model Hamiltonian to demonstrate the asymmetric line shape in organic crystals. The model of Klafter and Jortner is that every site has an excitation energy following a Gaussian distribution, whereas in our case we assume that all sites except a number n_d, n_d being a small fraction of the total, have the same excitation energy characteristic of an unperturbed structure. The n_d perturbed sites have trap depths Δ following a Gaussian distribution of half-width D and energies centered at C, the unperturbed band center being taken at energy zero. Thus the normalized distribution is

$$P(\Delta_p)=(2\pi D^2)^{-1/2}\exp[-(\Delta_p-C)^2/2D^2]\,, \qquad (4.9)$$

so that the most probable value of Δ_p is at $\Delta_p=C$.

Averaging (4.7) over (4.9) [multiply (4.7) by (4.9) and convert the sum into an integral] we find for the line shape

$$I_d(E)\propto -(2\pi D^2)^{-1/2}m^2[(E+B)^3/E^2(E-B)]^{1/2} \times\exp\{-[(E^2-B^2)^{1/2}-C]^2/2D^2\},\quad E<B<0\,. \qquad (4.10)$$

The following cases of particular interest will be considered.

Case (1): $|C|<|B|<|D|$. Here the width of the distribution of depths Δ is larger than that of the unperturbed band. This implies that, while the spread of depths is large, the most probable value lies within the unperturbed band. For $C=0.0$, $-0.5|B|$, and $0.5|B|$, the features of this case are illustrated, respectively, in Figs. 1(a), 1(b), and 1(c). In the region far below the band edge, for $|E|>|B|$ the preexponential factor in the square brackets of (4.10) is close to unity. The line shape $I(E)$ becomes Gaussian centered at C. Near the band edge, $E\sim B$, the limiting behavior is as $(E-B)^{-1/2}$. Except for the feature of our work allowing for the energy dependence of transition moment, the line shape derived in (4.10) for $C=0$ agrees with that calculated by Klafter and Jortner[9] in one-dimensional molecular crystals for the case that all sites are included in the Gaussian distribution. For distributions centered away from the midpoint of the band as shown in Figs. 1(a) and 1(c), the shapes of the tail vary little for the same distribution half-width D.

Case (2): $|C|>|B|<|D|$. In this case the traps are deep, with the mean trap level falling outside the unperturbed band, and the distribution is wide. Two examples with $C=-2|B|$ and $2|B|$ are illustrated in Figs. 1(d) and 1(e). Where the distribution of traps is centered below the band there is substantial absorption in the tail, and a small deviation from a smooth profile at $E\sim -4B$. With the distribution centered above the band the low-energy tail is weak and narrow [Fig. 1(e)].

Case (3): $|C|>|B|>|D|$. In this case the distribution of depths is centered outside the band, but is narrow. We show in Fig. 2 an example with $C=-1.5|B|$ and $D=0.5|B|$. As expected, the

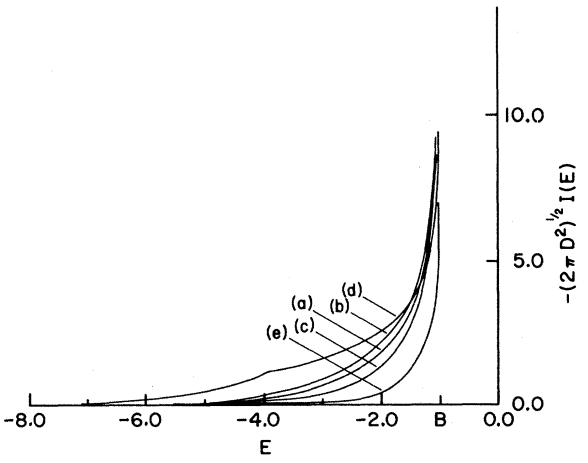

FIG. 1. Line shape of the low-energy tail of absorption calculated for crystals with one-dimensional tight-binding energy bands and for the ratio $D/B=2$; (a) $C=0.0$, (b) $C=-0.5|B|$, (c) $C=0.5|B|$, (d) $C=-2|B|$, and (e) $C=2|B|$.

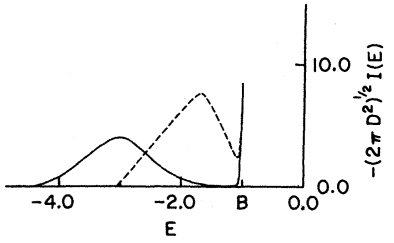

FIG. 2. Line shape of the low-energy tail calculated with the ratio $D/B=\frac{1}{2}$. —represents the tail for crystals with the Hubbard's type of the unperturbed density of states and $C=-3|B|$, and --- represents that for one-dimensional crystals with $C=-1.15|B|$.

spread of the tail is pushed out of the unperturbed band and shows a well-developed peak.

Case (4): $|C|$ and $|D| \ll |B|$. In this case the depths Δ are very small compared with the bandwidth, and thus all the energies E_α (4.3) are close to B. Let us, therefore, put $B-E=\delta$, where δ is small and positive. In this limit the line shape (4.10) becomes $(E+B \sim 2B)$

$$I_d(E) \propto -(2\pi D^2)^{-1/2} \tilde{m}^2 [8B/(E-B)]^{1/2} \times \exp(-\{[2B(E-B)]^{1/2}-C\}^2/2D^2), \quad E<B<0. \tag{4.11}$$

$I(E)$ from (4.11) is illustrated for $C=0$, $-0.5|B|$, and $0.5|B|$, respectively, in Figs. 3(a), 3(b), and 3(c). Here, unlike case (1), there is a difference between the line shapes with $C<0$ and $C>0$. While in the former, $C<0$, the tail is pushed out [Fig. 3(b)], in the latter this is pushed into [Fig. 3(c)] the exciton band.

In the case of $C=0$ [Fig. 3(a)] we find, for energies close to the band edge, a profile of the same form as in case (1), namely, an intensity rising much faster than a Gaussian function. At energies farther from the band edge where the intensities are extremely small the profile becomes proportional to $\exp[-B(E-B)/D^2]$, namely, exponential rather than Gaussian, as found in the Urbach-Martienssen rule for the low-energy absorption onset in alkali halides. This rule is given in (4.12):

$$I(E)=I_0 \exp[-\sigma(E-E_0)], \tag{4.12}$$

where I_0 is the intensity of absorption at the unperturbed band edge E_0. A comparison of (4.11) and (4.12) shows that in our calculation the steepness parameter $\sigma=B/D^2$. Sumi and Toyozawa[7] have estimated σ due to involvement of phonons for alkali halides as

$$\sigma=\eta B/S, \tag{4.13}$$

where

$$S=D^2/2k_BT.$$

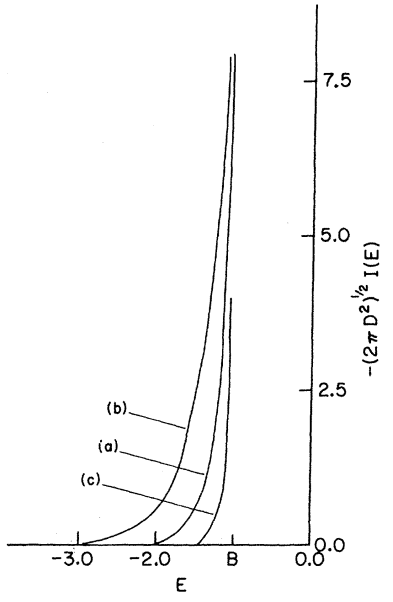

FIG. 3. The low-energy tail of absorption, similar to the U M tail, calculated for one-dimensional crystals with $D/B=\frac{1}{2}$, where (a) $C=0.0$, (b) $C=-0.5|B|$, and (c) $C=0.5|B|$.

In the present case, however, we have so far considered only the involvement of defects where S is expected to be a temperature-indpendent quantity.

B. More complex band structures

The density of states used for the one-dimensional crystal is realistic in examples where the coupling is to nearest neighbors only. In more complex cases model band structures and densities of states may be used or numerical calculations can be made from actual band characteristics known for particular systems. Our work in this and following sections is based on two model densities of states. The first is given in (4.14) and is due to Hubbard[11]:

$$N_0(E)=\begin{cases}(1/B)^2(2/\pi)(B^2-E^2)^{1/2} & \text{for } |E|<|B| \\ 0 & \text{for } |E|>|B|,\end{cases} \tag{4.14}$$

and the second is the uniform density of states, independent of energy within the band.

1. Hubbard's model of density of states

The density (4.14) has its maximum at the center of the band and goes to zero at the band edges. The unperturbed Green's function we then find to be

$$G_0(E)=N^{-1}\sum_k [E-E(\vec{k})]^{-1}=\int_{-B}^{B} \frac{N_0(E_0)dE_0}{E-E_0+i\epsilon}, \quad \epsilon \to 0$$
$$=2(1/B)^2[E-(E^2-B^2)^{1/2}]. \tag{4.15}$$

Substituting (4.15) in (3.8) the secular equation can be solved for energies E outside the band. Each value of trap depth $|\Delta_\rho|$ yields two solutions of (4.16a):

$$[E-(E^2-B^2)^{1/2}-2\Delta_\rho][E+(E^2-B^2)^{1/2}-2\Delta_\rho]=0. \tag{4.16a}$$

Alternatively, according to (4.16b) we find one solution below the band and one above, for negative and positive depths Δ_ρ respectively:

$$E=\Delta_\rho+B^2/4\Delta_\rho. \tag{4.16b}$$

While the first factor of (4.16a) gives energies ($E<0$) falling out of the lower band edge, the second factor produces energies symmetrically situated on the high-energy side ($E>0$) of the unperturbed band. The low-energy tail of absorption thus arises due to energy states obtained from the first factor of (4.16a) and the corresponding energy Green's function can then be calculated as in (4.6).

The transition moment corresponding to an energy E_α of (4.16a) can be calculated from (4.4) and (4.14) as

$$T_d(E_\alpha)=\frac{T}{E_\alpha-B}\left(\frac{2N[(E_\alpha^2-B^2)-E_\alpha]}{B^2(E_\alpha^2-B^2)^{1/2}}\right)^{-1/2}. \tag{4.17}$$

According to (4.7) we can then write

$$I_d(E)\propto-\frac{B^2}{2E[(1-B^2/E^2)^{1/2}-1]}\,\vec{m}\left(\frac{E+B}{E-B^3}\right)^{1/2}\times\sum_\rho\delta(E-E_{\alpha(\rho)}),\quad E<B, \tag{4.18}$$

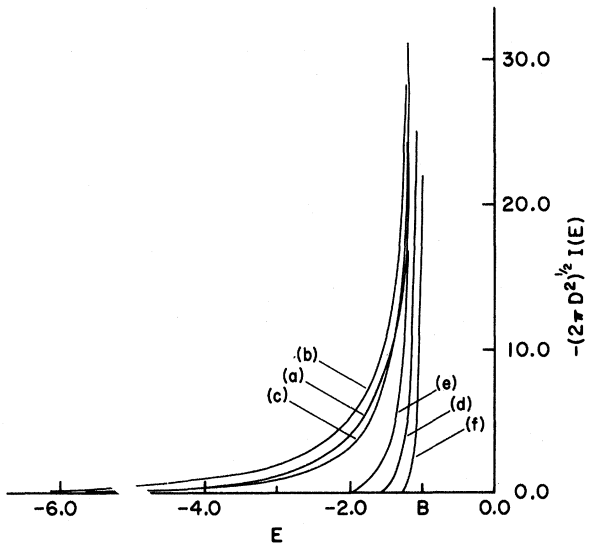

FIG. 4. Line shape of the low-energy tail calculated for crystals with Hubbard's density of states, where $D/B=2$ for (a) $C=0.0$, (b) $C=-0.5|B|$, and (c) $C=0.5|B|$, and $D/B=0.5$ for (d) $C=0.0$, (e) $C=-0.5|B|$, and (f) $C=0.5|B|$.

$$I_d(E)\propto-\frac{(2\pi D^2)^{-1/2}B^2}{2E[(1-B^2/E^2)^{1/2}-1]}\,\vec{m}^2\left(\frac{E+B}{(E-B)^3}\right)^{1/2}\times\exp\left(\frac{-\{\frac{1}{2}[E-(E^2-B^2)^{1/2}]-C\}^2}{2D^2}\right),\quad E<B<0. \tag{4.19}$$

The low-energy tail thus derived in (4.19) becomes Gaussian for $|E|>|B|$ and $|D|>|B|$ because then $(1-B^2/E^2)^{1/2}\sim 1-B^2/2E^2$, and the preexponential factor tends subsequently to unity. This is found for $I(E)$ in (4.10) as well. At energies not very far from the band edge, however, the rise of the tail (4.19) is steeper than that of (4.10) because both the preexponential and exponential factors of (4.19) rise steeper as E tends to B. We have shown the features of the tail in (4.19) in Figs. 2 and 4.

2. *Constant density of states*

In this case we assume that the unperturbed density of states N_0 is a constant quantity so that

$$N_0(E)=\begin{cases}\rho_0 & \text{for } |E|<|B|\\ 0 & \text{for } |E|>|B|.\end{cases} \tag{4.20}$$

Following (4.15) we then find the unperturbed energy Green's function as

$$G_0(E)=\rho_0\ln[(E+B)/(E-B)]+i\pi\rho_0, \tag{4.21}$$

so that

$$\frac{1}{\pi}\,\mathrm{Im}G_0(E)=\rho_0. \tag{4.22}$$

Using (4.21) in the secular equation (3.8) we find

$$1-\Delta_\rho\rho_0\ln\left(\frac{E+B}{E-B}\right)=0 \tag{4.23}$$

which yields the energy state outside the unperturbed exciton band at

$$E=B[\exp(1/\Delta_\rho\rho_\rho)+1]/[\exp(1/\Delta_\rho\rho_0)-1]. \tag{4.24}$$

The energy E from (4.24) tends toward the unperturbed band edge as $\Delta_\rho\to 0$. In order to obtain that $\Delta_\rho<0$ should yield the energies falling out of the lower band edge, we must have $\rho_0<0$.

The transition moment $T(E)$ corresponding to an energy state at E obtained from (4.24), is calculated from (4.4) and (4.20) as

$$T_d(E_\alpha)=TN^{-1/2}\left(\frac{E_\alpha+B}{E_\alpha-B}\right)^{1/2}. \tag{4.25}$$

Following now (4.7) we can write the line shape of the low-energy tail:

$$I_d(E)\propto-\vec{m}^2\left(\frac{E+B}{E-B}\right)\sum_\rho\delta(E_{\alpha(\rho)}-E). \tag{4.26}$$

The average of (4.26) over the Gaussian distribu-

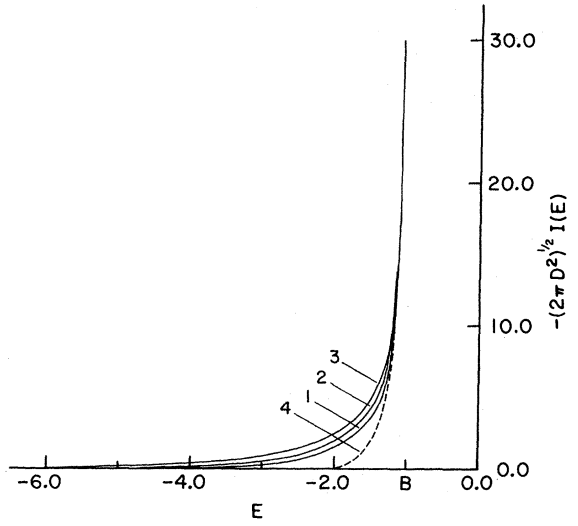

FIG. 5. Line shape of the low-energy tail calculated for crystals with uniform density of states $\rho_0 = 1/2B$. (1) $C = -0.5|B|$ and $D/B = 2$, (2) $C = 0.0$ and $D/B = 2$, (3) $C = 0.5|B|$ and $D/B = 2$, and (4) $C = -0.5|B|$ and $D/B = \frac{1}{5}$.

tion yields

$$I_d(E) \propto -\vec{m}^2 \left(\frac{E+B}{E-B}\right) \exp\left\{-\left[\frac{1}{\rho_0} \ln\left(\frac{E+B}{E-B}\right) - C\right]^2 / 2D^2\right\}. \tag{4.27}$$

We have shown $I(E)$ of (4.27) for $\rho_0 = 1/2B$ corresponding to (I) $D^2 > B^2$ and $|C| < |B|$, and (II) $D^2 < B^2$ and $|C| < |B|$ in Fig. 5.

V. COMBINED EFFECT OF CRYSTAL DEFECTS AND PHONONS ON THE LINE SHAPE

At higher temperatures the exciton absorption line shape will simultaneously be influenced by the exciton-defect and exciton-phonon interactions. In this section, therefore, we will derive the line-shape function from the complete Hamiltonian $\hat{H}_d$ (2.8) which comprises both the exciton-defect and exciton phonon-interactions. After transforming the Hamiltonian (2.8) with the help of (3.10) and (3.11), we can write it for a single defect site as given in (5.1):

$$H_d^{\rho} = \sum_{\alpha(\rho)} E_\alpha B_\alpha^\dagger B_\alpha + \sum_{\vec{q}} \hbar\omega(\vec{q})(b_{\vec{q}}^\dagger b_{\vec{q}} + \tfrac{1}{2}) + N^{-1/2} \sum_{\alpha,\alpha',\vec{q}} \left(\sum_{\vec{k}} [F(\vec{k},\vec{q}) + \chi(\vec{q})] A_{\vec{k}+\vec{q}}^{*}(\alpha) A_{\vec{q}}(\alpha')\right) \times B_\alpha^\dagger B_{\alpha'} (b_{-\vec{q}}^\dagger + b_{\vec{q}}). \tag{5.1}$$

In deriving H_d^{ρ} (5.1), the phonon part of the Hamiltonian (second term) is assumed unchanged by the presence of lattice defects in the crystal.

The Hamiltonian (5.1) suggests that its time Green's function $G(\alpha, t)$ can easily be evaluated by Iguchi's[16] method, and then the Fourier transform of $G(\alpha, t)$, calculated within the damping approximation,[14,19] yields the energy Green's function as given in (5.2):

$$G(\alpha, E) = \sum_{\rho} [E - E_{\alpha(\rho)} - \mathrm{Re}S(\alpha) + i\,\mathrm{Im}S(\alpha) + i\epsilon]^{-1}, \quad \epsilon \to 0, \tag{5.2}$$

where

$$\mathrm{Re}S(\alpha) = N^{-1} \sum_{\alpha',\vec{q}} C_{\alpha\alpha'}(\vec{q}) \left(\frac{\bar{\nu}_{\vec{q}}}{\Omega_{\alpha\alpha'}^{+}(\vec{q})} - \frac{1+\bar{\nu}_{\vec{q}}}{\Omega_{\alpha\alpha'}^{-}(\vec{q})}\right), \tag{5.3}$$

$$\mathrm{Im}S(\alpha) = \pi N^{-1} \sum_{\alpha',\vec{q}} C_{\alpha\alpha'}(\vec{q}) [\bar{\nu}_{\vec{q}} \delta(\Omega_{\alpha\alpha'}^{+}(\vec{q})) + (1+\bar{\nu}_{\vec{q}}) \delta(\Omega_{\alpha\alpha'}^{-}(q))], \tag{5.4}$$

$$C_{\alpha\alpha'}(\vec{q}) = \sum_{\vec{k}} [F(\vec{k},\vec{q}) + \chi(\vec{q})]^2 A_{\vec{k}+\vec{q}}^2(\alpha) A_{\vec{k}}^2(\alpha'), \tag{5.5a}$$

$$\Omega_{\alpha\alpha'}^{+}(\vec{q}) = E_\alpha - E_{\alpha'} + \hbar\omega(\vec{q}), \tag{5.5b}$$

$$\Omega_{\alpha\alpha'}^{-}(\vec{q}) = E_\alpha - E_{\alpha'} - \hbar\omega(\vec{q}), \tag{5.5c}$$

and

$$\bar{\nu}_{\vec{q}} = \{\exp[\beta\omega(\vec{q})] - 1\}^{-1}, \quad \beta = 1/k_B T. \tag{5.5d}$$

$\Omega_{\alpha\alpha'}^{+}(\vec{q})$ and $\Omega_{\alpha\alpha'}^{-}(\vec{q})$ represent, respectively, the increase and decrease in energy due to absorption or emission of a phonon with energy $\hbar\omega(\vec{q})$ during the scattering of the exciton from state α to α' by phonons.

E_α and $S(\alpha)$ both are functions of Δ_ρ; the difference in the defective-site energies from the normal. Substituting $A_{\vec{k}}(\alpha)$ from (3.12) in (5.5a) we can write $C_{\alpha\alpha'}(\vec{q})$ as

$$C_{\alpha\alpha'}(\vec{q}) = (N_\alpha N_{\alpha'})^{-2} \sum_{\vec{k}} \frac{[F(\vec{k},\vec{q}) + \chi(\vec{q})]^2}{[E_\alpha - E(\vec{k}+\vec{q})]^2 [E_{\alpha'} - E(\vec{k})]^2}. \tag{5.6}$$

$C_{\alpha\alpha'}(\vec{q})$ expressed in (5.6) is in a form that can be directly compared with the corresponding function derived for crystals with no defects.[14]

For calculating the line shape of absorption due to phonons we will assume that the transition moment $T_d(E)$ is independent of the phonon energy. In other words we assume that the transition moments corresponding to energy eigenvalues of (5.1) are the same as those used in Sec. IV, namely, $T_d(E)$ as in (4.5), (4.17), and (4.25) for three different cases of the unperturbed density of states.

From Eq. (5.2) we can then write the line-shape function as

$$I(E)\propto -\sum_{p}\frac{T_d^2[\mathrm{Im}S(\alpha)+\epsilon]}{[E-E_{\alpha(p)}-\mathrm{Re}S(\alpha)]^2+[\mathrm{Im}S(\alpha)+\epsilon]^2}\,,\quad E<B<0 \text{ and } \epsilon\to 0\,. \tag{5.7}$$

The expression (5.7) exhibits, for every p, a thermally broadened line shape of the tail which, depending on the strength of exciton-phonon coupling (weak or strong), becomes Lorentzian or Gaussian.[5,14]

A weighted average of (5.7) over the Gaussian distribution (4.9) yields

$$I(E)\propto -\frac{T_d^2\mathrm{Im}S(\alpha)}{[E-E_\alpha-\mathrm{Re}S(\alpha)]^2+[\mathrm{Im}S(\alpha)]^2}+\frac{I_d(E)}{[\mathrm{Re}S(\alpha)]^2+[\mathrm{Im}S(\alpha)+1]^2}\,,\quad E\ll B\,. \tag{5.8}$$

Equation (5.8) is derived by assuming that $S(\alpha)$ is independent of Δ_p; and ϵ can still be replaced by the $(1/\pi)\mathrm{Im}G(E,E_\alpha)=\delta(E-E_\alpha)$ calculated in the preceding section. For obtaining the first term of (5.8) we have neglected the dependence of E_α on Δ_p as it is expected to be smaller than $\mathrm{Re}S(\alpha)$. Equation (5.8) represents the line shape of the low-energy tail as a superposition of the line shape due to thermal broadening (first term) and that due to the exciton-defect interaction (the second term). At higher temperature the first term is dominant, giving rise to Lorentzian line shape whereas at low temperature the second term dominates to give rise to the asymmetric line shape. We can substitute E_α, T_d^2, and $I_d(E)$ from any one of the three cases considered in Sec. IV, namely, with (a) one-dimensional exciton energy band, (b) Hubbard density of states, and (c) constant density of states, to find the corresponding line shape of absorption from (5.8).

VI. DISCUSSION

The defects considered in this paper represent a change in the excitation energy only at some of the lattice sites of the crystal. In particular, we have introduced such defects in an otherwise perfect crystal by translational or orientational deviation of the equilibrium positions of some of the molecules. In principle, however, the theory is applicable to chemical impurities as well. The Hamiltonian (2.4), unlike the one considered by Klafter and Jortner,[9] contains the exciton-defect interaction term as a sum of the defect lattice sites only.

We have considered here three examples of the exciton energy bands, namely, (1) one-dimensional tight-binding, (2) with Hubbard's density of states, and (3) with energy-independent density of states for which the secular equation (3.8) can be solved exactly. Solutions thus obtained are, corresponding to every defect, the possible energy states beyond the edges of the unperturbed exciton band. We can, therefore, study the absorption due to transitions from the ground state to any of these excited energy states. All three examples for negative Δ_p have energy states lying below the bottom of the band and the corresponding transition, gives rise to a low-energy tail of absorption. In the method of t-matrix approximation[9] however, it is not possible to find the energy states explicitly as a function of Δ_p.

A. Influence of the defects

Calculation of the line shape as a weighted average over the Gaussian distribution of Δ_p, centered at an energy C from the center of the unperturbed band, is based on the assumption that the most probable value of Δ is C. There are three independent parameters B, C, and D which can influence the line-shape function. While C may be considered a measure of the homogeneity of the defects (Δ_p), D is considered a measure of the width of the distribution of defects. Thus C can be large even if D is small and one may find small C when D is very large. C and D cannot, however, be very large if Δ's are rather small, but D can be small even for large Δ.

In all three examples of crystals considered in this paper the low-energy tail appears to have similar shapes as can be seen in Figs. 1, 4, and 5 for $D^2\gg B^2$. This is due to our assumption that Δ's follow a Gaussian distribution, and implies that for $D^2>B^2$ it is the form of the distribution that dominates the line shape.

In Fig. 2 we have illustrated a special case of the tail, where for one-dimensional crystals we have used $C=-1.5|B|$ and $|D|=0.5|B|$, i.e., $|C|>|B|$ but $D^2<B^2$ and calculated from Eq. (4.10). Although here $D^2\ll B^2$, we cannot use Eq. (4.11) derived for small Δ or hence for small D, because the most probable value of Δ is $|C|>|B|$. The interesting feature of this case is that it shows a very distinct additional absorption peak at an energy $E\sim -1.8|B|$, where the exponential factor has its maximum. Likewise in three-dimensional crystals with Hubbard's model for the density of states and $C=-3|B|$, we find the additional peak at $E\sim -3.0|B|$ (Fig. 2). These peaks in Fig. 2 and the delta-function peak for identical Δ in (4.8) corresponds to the absorption due to the crystal defects of trap energy levels in the crystal and represent the localized states of excitons at energies $E<B$ (the trap depth C is larger than the kinetic energy

of the exciton).

Crystals with the constant unperturbed density of states show that the line shape (4.27) has one of the features particularly different from those of the previous two examples. The influence of C, the most probable value of Δ, on the low-energy tail is not very significant. For instance, when $|C|<|B|$ the value of C can affect the line shape of the tail only at energies close to the band edge where the preexponential factor, which is independent of C, becomes dominant (see 4.27). On the other hand, when $|C|>|B|$ the influence of C on the line shape can be noticeable at $|E|>|B|$ where $\ln[(E+B)/(E-B)]$ tends to zero. As a result the exponential part of (4.27) depends more on $(1/\rho_0)\ln[(E+B)/(E-B)]$ than on C. Unlike the other two cases of the density of states, therefore, we have not found here a well-defined additional peak due to defects in the low-energy tail.

B. U M tail

1. One-dimensional crystals

As a result of $|\Delta|$ being very small the magnitudes of $|D|$ and $|C|$ have to be small, and then the limiting line-shape function becomes derived as in (4.11). Most of the contributions to the low-energy tail, therefore, come from energies close to the edge of the unperturbed band where the rise of the tail is much steeper than a Gaussian. The observed asymmetric line shape in the absorption spectra of 1,4-DBN crystals[1] does show a steep rise of the low-energy tail at a temperature 2 K, similar to those shown in Fig. 3. The line shape shown in Fig. 3(c) for $C=0.5|B|$ has a rise steeper than that of the Fig. 3(a) for $C=0.0$ and Fig. 3(b) for $C=-0.5|B|$. As Δ's are regarded small, it is very likely that C will be close to zero which implies that the line-shape curves of Fig. 3(a) may be expected to represent the observed line shape. A more precise comparison of the present theory with experiment, however, requires the knowledge of the ratios of D to B and C to B for which no experimental data are available.

Another argument in favor of Eq. (4.11) being possibly the correct representation of the asymmetric tail in DBN crystals is the exponential dependence of $I(E)$ on E that represents the correct Urbach-Martienssen tail[7] with the steepness parameter $\sigma=B/D^2$ for $C=0$ and the temperature-independent D.

In organic crystals of large molecules, DBN for example, such defects (due to translational or orientational displacements of the lattice sites, as considered here) can possibly always grow with the cyrstals in the form of small changes in the orientations of even a part of the molecules. Consequently, the distribution of such defects in crystals can vary from one to another even if they are grown in the same laboratory. Subsequently the degree of asymmetry in the line shape can also vary from crystal to crystal of the same material. This explains the results on 1,4-DBN crystals by Burland and Macfarlane[2] and Peretti and Ranson[20] observed independently. Peretti and Ranson have observed more asymmetric line shape than that observed by the former workers.

2. Three-dimensional crystals

In case of small trap depths the line shape (4.19) for exciton bands with Hubbard's density of states reduces to

$$I(E)\propto\frac{B^2}{|E|}[2B/(E-B)^3]^{1/2}\exp[-(E-2C)^2/8D^2]\,. \tag{6.1}$$

Considering that this condition represents the UM tail at a particular value of C, say $C=0$, we find that $I(E)$ in (6.1) rises much faster than that in (4.11) (see Figs. 3 and 5).

Klafter and Jortner[9] have calculated the UM tail arising due to the static disorder for exciton bands with unperturbed density of states of the Hubbard's type. Their results are derived through the application of single-site average t-matrix approximations (ATA) for $D^2\ll B^2$ and $C=0$. The exponential dependence of $I(E)$ in (4.19) is in agreement with that derived by Klafter and Jortner.

The exciton bands with constant density of states are expected to have UM tails as shown in Fig. 5, with (4) corresponding to $D^2\ll B^2$. The rise of the tail is found to be faster than the corresponding line shapes of the other two examples as shown in Figs. 3 and 4.

C. Combined effect of defects and phonons

As shown in (5.1) the presence of crystal defects modifies the usual exciton-phonon interaction operator in a perfect crystal.[12] Thus the presence of defects gives rise not only to the asymmetric tail (Sec. IV) of absorption but also modifies the thermal broadening due to phonons.

At higher temperatures the effect of phonons is dominant and the line shape observed is primarily due to thermal broadening. Consequently the asymmetry in the line shape, caused by the crystal defects, is expected to disappar at higher temperatures. This has been observed in the 1,4-DBN crystals at 25 K; the line shape of absorption becomes symmetric and Lorentzian. It would probably be of academic interest to observe the critical temperature at which such a transition takes place. If both interactions, exciton-defect and exciton-

phonon, are strong, the line shape of the tail will be Gaussian due to both defects (4.19) and phonons.[14] Depending thus on the values of C and D the combined effect of defects and phonons will then be added together, but the line shape will remain Gaussian.

The theory presented in this paper corresponds to situations where the optical transitions are very weak and exciton-photon interactions can be omitted. However, in crystals where the transitions are strong exciton-photon interaction gives rise to polaritons which exhibit rather complicated line shapes of absorption.[21] A theory encountering the interactions of polariton-defects and polariton-phonons is not yet fully developed. Work is in progress in this direction.

ACKNOWLEDGMENTS

I am indebted to Professor D. P. Craig for many valuable suggestions and comments regarding the contents and improvements in this paper, and thanks are due Dr. J. Mahanty for several discussions.

---

[1]D. M. Burland, J. Chem. Phys. 59, 4283 (1973).
[2]D. M. Burland and R. G. Macfarlane, J. Lumin. 12, 213 (1976).
[3]F. Urbach, Phys. Rev. 92, 1324 (1953).
[4]W. Martienssen, J. Phys. Chem. Solids 2, 257 (1957).
[5]Y. Toyozawa, Prog. Theor. Phys. 20, 53 (1956); 27, 89 (1962).
[6]A. S. Davydov and E. N. Myasnikov, Phys. Status Solidi 20, 153 (1967).
[7]H. Sumi and Y. Toyozawa, J. Phys. Soc. Jpn. 31, 342 (1971).
[8]L. A. Dissado, Chem. Phys. 8, 289 (1975).
[9]J. Klafter and I. Jortner, Chem. Phys. 26, 421 (1977); J. Chem. Phys. 68, 1513 (1978).
[10]J. Singh. J. Lumin. 18, 461 (1979).
[11]J. Hubbard, Proc. R. Soc. London A277, 237 (1964); A281, 401 (1964).
[12]A. S. Davydov, *Theory of Molecular Excitons* (Plenum, New York, 1971).
[13]Δ_p, derived in the form of (2.5), is a result of the assumption that the displacement ρ is small and we could, therefore, make the Taylor's expansion of $\hat{H}$ about the equilibrium positions in the perfect lattice. If, however, the p values are not small, one should do the expansion about the displaced equilibrium position. Δ_p is then simply obtained as the change in the dispersive interactions $[\Delta_p = D_{pm}(\rho) - D_{pm}(0)]$ due to the displacement of the equilibrium sites.
[14]D. P. Craig and L. A. Dissado, Chem. Phys. 14, 1976 (1976).
[15]R. M. Hochstrasser and P. N. Prasad, in *Excited States*, edited by E. C. Lim (Academic, New York, 1974), Vol. 1, p. 79.
[16]K. Iguchi, J. Chim. Phys. 71, 654 (1974).
[17]D. P. Craig and M. R. Philpott, Proc. R. Soc. London A290, 583 (1966); A290, 602 (1966); A293, 213 (1966).
[18]G. F. Koster and J. C. Slater, Phys. Rev. 95, 1167 (1954).
[19]W. Heitler, *Quantum Theory of Radiation*, 3rd ed. (Oxford University Press, London, 1954).
[20]P. Peretti and P. Ranson (unpublished spectrum).
[21]J. Ferguson, Z. Phys. Chem. 101, 45 (1976).